The Journal of Immunology

Oxidized Low-Density Lipoprotein Loading of Macrophages Downregulates TLR-Induced Proinflammatory Responses in a Gene-Specific and Temporal Manner through Transcriptional Control

Jenny Jongstra-Bilen, Cindy X. Zhang, Timothy Wisnicki, Mengyi K. Li, Samantha White-Alfred, Ragave Ilaalagan, Dario M. Ferri, Ashley Deonarain, Mark H. Wan, Sharon J. Hyduk, Carolyn L. Cummins and Myron I. Cybulsky

J Immunol 2017; 199:2149-2157; Prepublished online 7 August 2017;
doi: 10.4049/jimmunol.1601363
http://www.jimmunol.org/content/199/6/2149

The Journal of Immunology is published twice each month by
The American Association of Immunologists, Inc.,
1451 Rockville Pike, Suite 650, Rockville, MD 20852

Print ISSN: 0022-1767 Online ISSN: 1550-6606.

Oxidized Low-Density Lipoprotein Loading of Macrophages Downregulates TLR-Induced Proinflammatory Responses in a Gene-Specific and Temporal Manner through Transcriptional Control

Jenny Jongstra-Bilen,*,†,‡ Cindy X. Zhang,*,‡ Timothy Wisnicki,*,‡ Mengyi K. Li,*,† Samantha White-Alfred,* Ragave Ilaalagan,*,† Dario M. Ferri,*,‡ Ashley Deonarain,*,‡ Mark H. Wan,* Sharon J. Hyduk,* Carolyn L. Cummins,§ and Myron I. Cybulsky*,†,‡

Hypercholesterolemia is a key risk factor for atherosclerosis and leads to the uptake of native and oxidized low-density lipoprotein (oxLDL) by macrophages (Mϕs) and foam cell formation. Inflammatory processes accompany Mϕ foam cell formation in the artery wall, yet the relationship between Mϕ lipid loading and their response to inflammatory stimuli remains elusive. We investigated proinflammatory gene expression in thioglycollate-elicited peritoneal Mϕs, bone marrow–derived Mϕs and dendritic cells, and RAW264.7 cells. Loading with oxLDL did not induce peritoneal Mϕ apoptosis or modulate basal-level expression of proinflammatory genes. Upon stimulation of TLR4, the rapid induction of IFN-β was inhibited in cells loaded with oxLDL, whereas the induction of other proinflammatory genes by TLR4 (LPS), TLR3 (polyriboinosinic-polyribocytidylic acid), TLR2 (Pam_3CSK_4), and TLR9 (CpG) remained comparable within the first 2 h. Subsequently, the expression of a subset of proinflammatory genes (e.g., IL-1β, IL-6, CCL5) was reduced in oxLDL-loaded cells at the level of transcription. This phenomenon was partially dependent on NF erythroid 2–related factor 2 (NRF2) but not on nuclear liver X receptors α and β (LXRα,β), peroxisome proliferator-activated receptor-γ (PPARγ), and activating transcription factor 3 (ATF3). LPS-induced NF-κB reporter activity and intracellular signaling by NF-κB and MAPK pathways were comparable in oxLDL-loaded Mϕs, yet the binding of p65/RelA (the prototypic NF-κB family member) was reduced at IL-6 and CCL5 promoters. This study revealed that oxLDL loading of Mϕs negatively regulates transcription at late stages of TLR-induced proinflammatory gene expression and implicates epigenetic mechanisms such as histone deacetylase activity. ***The Journal of Immunology*****, 2017, 199: 2149–2157.**

Atherosclerosis is a chronic inflammatory disease characterized by the accumulation of macrophages (Mϕs) and oxidized low-density lipoprotein (oxLDL) in the intimal layer of elastic and muscular arteries (1, 2). Mϕs in atherosclerotic lesions accumulate intracellular lipid and become foam cells (3). In fact, resident intimal myeloid cells become foam cells within days of feeding LDL receptor deficient ($Ldlr^{-/-}$) mice a cholesterol-rich diet (4), and this precedes increased monocyte recruitment (5). It is widely accepted that Mϕ lipid loading is associated with proinflammatory gene expression that promotes monocyte recruitment and propagates lesion development (1, 6). Because Mϕ foam cells and inflammation persist throughout atherogenesis (7) and lesion formation can be regulated by Mϕ homeostasis (8, 9), it is important to understand how Mϕ lipid loading influences proinflammatory gene expression.

Incubation with oxLDL is a reproducible way for lipid loading of cultured Mϕs that take up modified lipoproteins through several routes, including scavenger receptors (CD36 and Msr1/SRA), macropinocytosis, and efferocytosis of apoptotic cells (10–12). The relative contribution of each in atherosclerosis is unknown and may depend on the age of the lesion. Oxidative modification of LDL and uptake into Mϕ have been implicated as a pathogenic process in atherosclerosis, and natural IgM Abs that bind oxLDL and moieties found on apoptotic cells serve as a protective mechanism (13, 14).

TLR4 is the receptor for bacterial endotoxin or LPS. LPS and inflammatory cytokines activate Mϕ intracellular signaling, including NF-κB and MAPK pathways, and profoundly induce proinflammatory gene expression (15, 16). TLR4 also has endogenous

*Toronto General Hospital Research Institute, University Health Network, Toronto, Ontario M5G 1L7, Canada; †Department of Laboratory Medicine and Pathobiology, University of Toronto, Toronto, Ontario M5S 1A8, Canada; ‡Department of Immunology, University of Toronto, Toronto, Ontario M5S 1A8, Canada; and §Leslie Dan Faculty of Pharmacy, University of Toronto, Toronto, Ontario M5S 3M2, Canada

ORCIDs: 0000-0003-2174-2217 (J.J.-B.); 0000-0002-0243-7842 (C.X.Z.); 0000-0001-6915-9018 (M.K.L.); 0000-0002-5637-8569 (R.I.); 0000-0002-0483-5529 (D.M.F.); 0000-0002-9519-2222 (A.D.); 0000-0001-7603-6577 (C.L.C.); 0000-0002-1696-2867 (M.I.C.).

Received for publication August 5, 2016. Accepted for publication July 16, 2017.

This work was supported by Canadian Institutes of Health Research Grants MOP 84446 and MOP 106522 (to M.I.C.) and Heart and Stroke Foundation of Canada Grant G-13-0002612 (to C.L.C.).

Address correspondence and reprint requests to Dr. Jenny Jongstra-Bilen, Toronto General Hospital Research Institute, University Health Network, 101 College Street, MBRC 2R-402R9, Toronto, ON M5G 1L7, Canada. E-mail address: jenny.jongstra.bilen@utoronto.ca

The online version of this article contains supplemental material.

Abbreviations used in this article: acLDL, acetylated LDL; ATF3, activating transcription factor 3; BMDC, bone marrow–derived DC; BMMϕ, bone marrow–derived Mϕ; ChIP, chromatin immunoprecipitation; DC, dendritic cell; DiI, 1,1′-dioctadecyl-3,3,3′,3′-tetramethylindocarbocyanine perchlorate; HDAC, histone deacetylase; hnRNA, heterologous nuclear RNA; HO-1, hemeoxygenase-1; LDL, low-density lipoprotein; LXR, liver X receptor; Mϕ, macrophage; NRF2, NF erythroid 2–related factor 2; ox, oxidized; PI, propidium iodide; PMϕ, peritoneal Mϕ; poly(I:C), polyriboinosinic-polyribocytidylic acid; PPARγ, peroxisome proliferator–activated receptor-γ; qPCR, quantitative PCR; TRAM, TRIF-related adaptor molecule; TRIF, Toll/IL-1R domain–containing adaptor inducing IFN-β; TSA, trichostatin A; wt, wild-type; ZnPP, zinc protoporphyrin.

www.jimmunol.org/cgi/doi/10.4049/jimmunol.1601363

ligands. For example, oxLDL binds CD36/TLR4/TLR6 complex and upregulates Mϕ proinflammatory gene expression (17). However, the magnitude of the oxLDL response is modest relative to LPS, and some studies have failed to observe enhanced proinflammatory gene expression (18, 19). Several studies have implicated TLR4 in atherosclerosis. TLR4-deficient mice are protected from atherosclerosis (20), and the importance of Mϕ TLR4 was demonstrated by reduced lesion area in mice reconstituted with bone marrow deficient in TLR4 or its adaptors, Toll/IL-1R domain–containing adapter-inducing IFN-β (TRIF) and TRIF-related adaptor molecule (TRAM) (21, 22). Polymorphisms in the TLR4 locus are associated with atherosclerosis in humans (23, 24). It remains to be determined whether TLR4 engagement with oxLDL or with other atherogenic ligands is relevant to lesion formation (20, 25). TLR3, TLR2, and TLR9 have also been implicated in atherosclerosis (22, 26).

Lipid-loaded peritoneal Mϕs (PMϕs) isolated from low-density lipoprotein receptor–deficient ($Ldlr^{-/-}$) mice fed a cholesterol-rich diet exhibited diminished proinflammatory gene expression in response to TLR4 signaling, as did PMϕs loaded in vitro with cholesterol (not oxLDL) (27). This study suggested that Mϕ cholesterol loading confers an anti-inflammatory phenotype. Hypercholesterolemia downregulated dendritic cell (DC) functions and inflammatory gene expression in vivo and in vitro in oxLDL-loaded cells stimulated with TLR ligands (28–30). These data suggest negative regulation of proinflammatory gene expression in lipid-loaded myeloid cells; however, the mechanism of this phenomenon is poorly understood. Desmosterol, a precursor of cholesterol biosynthesis, and nuclear liver X receptors (LXR) α and β have been implicated (27).

Peroxisome proliferator–activated receptor-γ (PPARγ) and LXRα/β are nuclear receptors activated by oxidized fatty acid ligands and metabolites of cholesterol (oxysterols), respectively. These nuclear receptors act as sensors of intracellular cholesterol, activated by Mϕ loading with oxLDL, to induce collectively the expression of genes involved in cholesterol metabolism and reverse cholesterol transport (31–34). Additionally, they exert a negative regulatory effect on TLR-induced Mϕ proinflammatory responses and atherosclerosis. Activation of LXRα/β or PPARγ inhibits TLR4-induced NF-κB activity by preventing the removal of nuclear receptor corepressor complexes from NF-κB regulatory sequences (31, 35–38). Activating transcription factor 3 (ATF3) is a member of the CREB family of basic leucine zipper transcription factors and has been implicated in the regulation of both inflammatory and lipid metabolic pathways (39, 40). ATF3 is a negative regulator of TLR4-mediated IL-6 and IL-12 expression and histone H4 acetylation in Mϕs (41). Additionally, ATF3 is a regulator of type I IFN–induced cholesterol 25-hydroxylase, which catalyzes the synthesis of the oxysterol 25-hydroxy cholesterol, a regulator of inflammasomes (42). ATF3 deficiency in apolipoprotein E–deficient ($ApoE^{-/-}$) mice results in more severe atherosclerosis than wild-type (wt) with increased lesion formation and 25-hydroxy cholesterol levels (39). The oxidative stress–induced transcription factor, NF erythroid 2–related factor 2 (NRF2), which encodes antioxidant genes and downregulates NF-κB–dependent proinflammatory gene expression, was reported to be atheroprotective in hypercholesterolemic $Ldlr^{-/-}$ mice but proatherogenic on $ApoE^{-/-}$ background, likely due to systemic effects on lipid metabolism (43–45).

We undertook to investigate whether oxLDL loading of Mϕs modulates their inflammatory response. Culturing of Mϕs with oxLDL for over 24 h did not alter proinflammatory gene expression by itself; however, the expression of a proinflammatory gene subset in response to TLR4, TLR3, TLR2, and TLR9 signaling was repressed in a time-dependent manner. The induction of LPS-induced transcription within the first 2 h was mostly unchanged, whereas transcription was reduced at later time points. The inhibition of LPS-induced gene expression by oxLDL was partially dependent on NRF2, but independent of LXR/PPARγ and ATF3. Although TLR4-induced NF-κB reporter activity and NF-κB signaling were not altered, NF-κB RelA/p65 subunit binding to proinflammatory gene promoter regions was reduced, implicating an epigenetic mechanism such as altered histone deacetylase (HDAC) activity.

Materials and Methods

Mice and cells

All mice were fed a standard rodent chow and all procedures were performed according to the guidelines of the Canadian Council on Animal Care and approved by Animal Care Committees. C57BL/6 (wt) and $Nrf2^{-/-}$ mice were from The Jackson Laboratory (Bar Harbor, ME), and $Atf3^{-/-}$ mice were from Dr. T. Hai (Ohio State University). These mice were housed at the University Health Network. LXRα/β$^{-/-}$ mice ($Nr1h3^{-/-}$ $Nr1h2^{-/-}$, backcrossed to the C57BL/6 strain for >10 generations) and corresponding wt mice (from Dr. D. Mangelsdorf, University of Texas Southwestern Medical Center, Dallas, TX) were housed at the University of Toronto. PMϕs were harvested 4 d after i.p. injection of 1 ml of 4% aged thioglycollate (BD Biosciences, Franklin Lakes, NJ) by lavage with cold PBS containing 2% FBS. Cells were cultured (37°C, 5% CO_2) for 3–18 h in growth media: (DMEM; Wisent Bio Products, Saint-Jean-Baptiste, QC, Canada) containing 10% FBS, 2 mM L-glutamine, and 10,000 U/ml penicillin/streptomycin (Life Technologies, Carlsbad, CA). Adhered PMϕs were used in experiments. Bone marrow–derived Mϕs (BMMϕs) and bone marrow–derived DCs (BMDCs) were prepared by standard methods using 20–40 ng/ml M-CSF and 10 ng/ml GM-CSF (PeproTech), respectively (46, 47). In some experiments, 20% L929 cell–conditioned medium was used instead of purified M-CSF. BMMϕs and BMDCs were assessed by flow cytometry for CD11b/F4/80 and CD11c/CD11b/MHC class II expression, respectively. The RAW264.7 murine Mϕ cell line was used below passage 20.

Reagents and Abs

Medium human oxLDL, acetylated LDL (acLDL), and 1,1′-dioctadecyl-3,3,3′,3′-tetramethylindocarbocyanine perchlorate (DiI) medium oxLDL were purchased from Kalen Biomedical (Germantown, MD). Ultrapure LPS, DNA containing CpG motif (oligodeoxynucleotide 1826), and trichostatin A (TSA) were from InvivoGen (San Diego, CA); polyriboinosinic-polyribocytidylic acid [poly(I:C)], cholesterol, and rosiglitazone were from Sigma-Aldrich (Oakville, CA); Pam_3CSK_4 and zinc protoporphyrin (ZnPP) IX were from Tocris Bioscience (Minneapolis, MN); and T0070907 was from Selleckchem (Boston, MA). For chromatin immunoprecipitation (ChIP) assays, p65 Ab (sc-372x) was from Santa Cruz Biotechnology (Dallas, TX) and rabbit IgG was from Jackson ImmunoResearch Laboratories (West Grove, PA). Primary Abs for Western blotting, anti-IκBα (L35A5), phosphorylated-specific mAbs NF-κB p65 (Ser^{536}, 93H1), p44/42 MAPK (Thr^{202}/Tyr^{204}, D13.14.4E), p38 MAPK (Thr^{180}/Tyr^{182}, D3F9), and SAPK/JNK (Thr^{183}/Tyr^{185}, 81E11), as well as loading control Abs anti–NF-κB p65 (D14E12), p44/42 MAPK (137F5), p38 MAPK (D13E1), and SAPK/JNK (56G8) were from Cell Signaling Technology (Danvers, MA), and anti–β-actin was from Sigma-Aldrich. HRP-conjugated secondary Abs were from Cell Signaling Technology or Jackson ImmunoResearch Laboratories.

Lipid loading and stimulation

Primary Mϕs (1×10^6) or RAW264.7 cells (0.25×10^6) were cultured in 24-well plates with or without oxLDL (100 μg/ml, 24 h) prior to stimulation (duration indicated) with LPS (100 ng/ml), poly(I:C) (100 μg/ml), Pam_3CSK_4 (10 ng/ml), or CpG (300 nM). The extent and uniformity of lipid loading was assessed by microscopy and flow cytometry. Confocal microscopy (FluoView 1000; Olympus) was carried out after paraformaldehyde (4%) fixation of cells on glass coverslips. Neutral lipid was stained with Nile Red (2.5 μg/ml; Sigma-Aldrich) and nuclei were counterstained with Hoechst 33342 (20 μg/ml; Invitrogen). Coverslips were mounted with Dako fluorescent mounting media (Dako, Santa Clara, CA). Flow cytometry (BD LSR II) was performed using trypsin (TrypLE; Life Technologies)–harvested cells 24 h after culture with a mixture of DiI-oxLDL and oxLDL (10 and 90 μg/ml, respectively). Cholesterol loading, that is, 24 h

culture with cholesterol (50 μg/ml), was assessed by confocal microscopy of filipin (Sigma-Aldrich)-stained fixed cells.

RNA isolation and quantitation by reverse transcription quantitative PCR

RNA isolation (E.Z.N.A. total RNA; Omega Bio-Tek, Norcross, GA) and reverse transcription (High Capacity RT Kit; Life Technologies) were performed according to the manufacturers' protocols. Primers that span over two successive exons were used for mRNA measurements. For heterogeneous nuclear RNA (hnRNA) measurements primers that amplify intron regions were designed and RNA was purified further by DNase I (200U/ml; Ambion) digestion. Real-time quantitative PCR (qPCR) was performed in triplicates using a Roche LightCycler 480 with SYBR master mix I (Roche), and quantification of relative amounts of mRNA and hnRNA were performed by the comparative standard curve method and normalized to the housekeeping gene hypoxanthine phosphoribosyltransferase mRNA and hnRNA, respectively. Primer sequences are in Supplemental Table I.

NF-κB luciferase reporter assays

The pGL4.32[luc2P/NF-κB-RE/Hygro] reporter vector (Promega, Madison, WI) contains five copies of NF-κB response elements inserted to the promoter region of the luciferase cDNA (NF-κB–firefly luciferase). Ub6–β-galactosidase (from Dr. C. Glass, University of California, San Diego, CA) or CMV–*Renilla* luciferase (from Dr. J. Fish, University Health Network) was used as normalizing internal controls in RAW264.7 cell and BMMϕ experiments, respectively. RAW264.7 cells (0.2×10^6) were cotransfected (SuperFect transfection reagent; Qiagen) with NF-κB–firefly luciferase (0.5 μg) and Ub6–β-galactosidase (0.1 μg) reporter plasmids. BMMϕs (2.5×10^6) were cotransfected (Amaxa Nucleofector and Cell Line Nucleofector kit V; Lonza, Allendale, NJ) with NF-κB–firefly luciferase (3.0 μg) and CMV–*Renilla* luciferase (0.1 μg). Luciferase activities were determined with β-Glo or Dual-Luciferase reporter systems (Promega) for RAW264.7 cells or BMMϕs, respectively, using a GloMax 20/20 luminometer (Promega).

ChIP

p65 ChIP was performed as described (27) with minor modifications. Nuclear lysate from 8×10^6 RAW264.7 cells was prepared for each immunoprecipitation and after shearing the DNA. Input sample lysate (1%) was retained. Immunoprecipitations were performed with Abs against p65 or rabbit IgG coupled to Dynabeads protein A (Novex; Thermo Scientific, Burlington, ON, Canada). DNA was isolated using the QIAquick PCR purification kit (Qiagen) according to the manufacturer's instructions, and qPCR was performed using primers specific for the promoters of indicated genes (Supplemental Table I). Enrichment of p65 and IgG control were calculated from copy numbers based on standard curves of genomic DNA as p65/input and IgG/input, respectively.

Western blotting

RAW264.7 cells (0.5×10^6) or PMϕs (2×10^6) were cultured overnight in 12-well plates and oxLDL loaded (100 μg/ml, 24 h) or control cells were stimulated with LPS (100 ng/ml, duration indicated) and lysed ($5–7 \times 10^6$/ml) directly in ice-cold RIPA buffer (1% Nonidet P-40, 0.1% SDS, 0.5% sodium deoxycholate in PBS) supplemented with 1 mM PMSF and cOmplete, mini, EDTA-free protease inhibitor cocktail (Roche) prior to dilution with 2× Laemmli sample buffer (Bio-Rad Laboratories, Hercules, CA) containing 2-ME. Cell lysates underwent SDS-PAGE (10–12% gels) and electrotransfer onto polyvinylidene difluoride membranes. Individual blots were first probed with phosphorylated-specific Abs before stripping and reprobing with Abs against total protein or actin, as indicated. Blots were developed using ECL chemiluminescence substrate (GE Healthcare, Pittsburgh, PA).

ELISA

The Ready-SET-Go! kit from eBioscience was used as per kit instructions to measure the levels of secreted IL-6, TNF-α, and MCP-1 in the supernatants of Mϕ cultures. The plates were read at OD 450 nm in the DTX 880 multimode detector (Beckman Coulter). Secreted IL-12 p40 and p70 levels were determined by Millipore/Sigma-Aldrich mouse 32plex immunology multiplex assay.

Analysis of apoptosis

Trypsin-harvested single-cell PMϕ suspensions were stained using the Annexin V^{FITC} apoptosis detection kit (eBioscience) and propidium iodide (PI) according to the manufacturer's instructions. Data (10^4 total events collected on a BD LSR II cytometer) were analyzed using FlowJo v10 software.

Statistical analyses

Two groups were compared using a two-tailed Student *t* test, and ANOVA and Tukey or Dunnett posttests compared multiple groups or fold increases over untreated cells, respectively (InStat3 and Prism5; GraphPad Software, La Jolla, CA).

Results

Loading of PMϕs with oxLDL does not induce proinflammatory gene expression

Two approaches were used to evaluate PMϕ lipid uptake after incubation with oxLDL. Confocal microscopy of Nile Red–stained cells showed abundant lipid droplets (Fig. 1A), and flow cytometry of cells cultured with DiI-labeled oxLDL showed accumulation in all cells (Fig. 1B). PMϕs loaded with oxLDL upregulated the expression of antioxidant genes, hemeoxygenase-1 (HO-1), sulforedoxin-1 (SRXN-1), and thioredoxin reductase-1 (TXNRD-1) (48), as well as the scavenger receptor CD36 (Fig. 1C), consistent with previous studies (34, 36). In contrast, the expression of proinflammatory genes was not increased in oxLDL-loaded PMϕs (Fig. 1C). Culture of Mϕs with oxLDL can induce apoptosis in serum-free medium or under conditions that induce endoplasmic reticulum stress (49–51); however, this was not observed with PMϕs under our experimental conditions (Fig. 1D). Incubation with indomethacin (52) served as a positive control.

OxLDL loading downregulates a subset of TLR-induced proinflammatory genes in a time-dependent manner

TLRs provide potent proinflammatory stimuli to myeloid cells. We examined whether oxLDL loading would modulate the expression of proinflammatory genes induced by TLR4, 3, 2 and 9 ligands [LPS, poly(I:C), Pam_3CSK_4, and CpG, respectively]. Within 2 h of

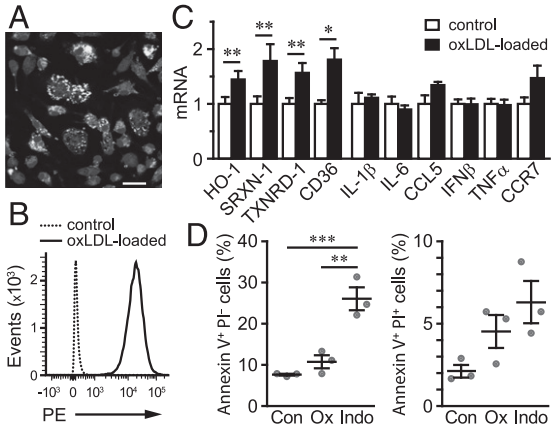

FIGURE 1. Loading of PMϕs with oxLDL (100 μg/ml) induces antioxidant genes and CD36, but not proinflammatory gene expression or apoptosis. (**A**) Abundant lipid droplets in oxLDL-loaded PMϕs are evident by confocal microscopy. Scale bar, 50 μm. (**B**) Flow cytometry histograms of PMϕs cultured with (black line) or without (control) DiI-oxLDL (see *Materials and Methods*). Representative data from one of four experiments are shown in (A) and (B). (**C**) PMϕs were cultured for 30 h with or without oxLDL, and mRNA expression was assessed by qPCR. oxLDL levels are expressed relative to control, which was designated as 1 (mean ± SEM, $n = 4$). (**D**) PMϕs were cultured for 30 h alone (Con), with oxLDL (Ox), or with 0.5 mM indomethacin (Indo). Flow cytometry assessed the percentage of cells in early (annexin V^+PI^-) and late (annexin V^+PI^+) stages of apoptosis (mean ± SEM, $n = 3$). $^*p < 0.05$, $^{**}p < 0.01$, $^{***}p < 0.001$.

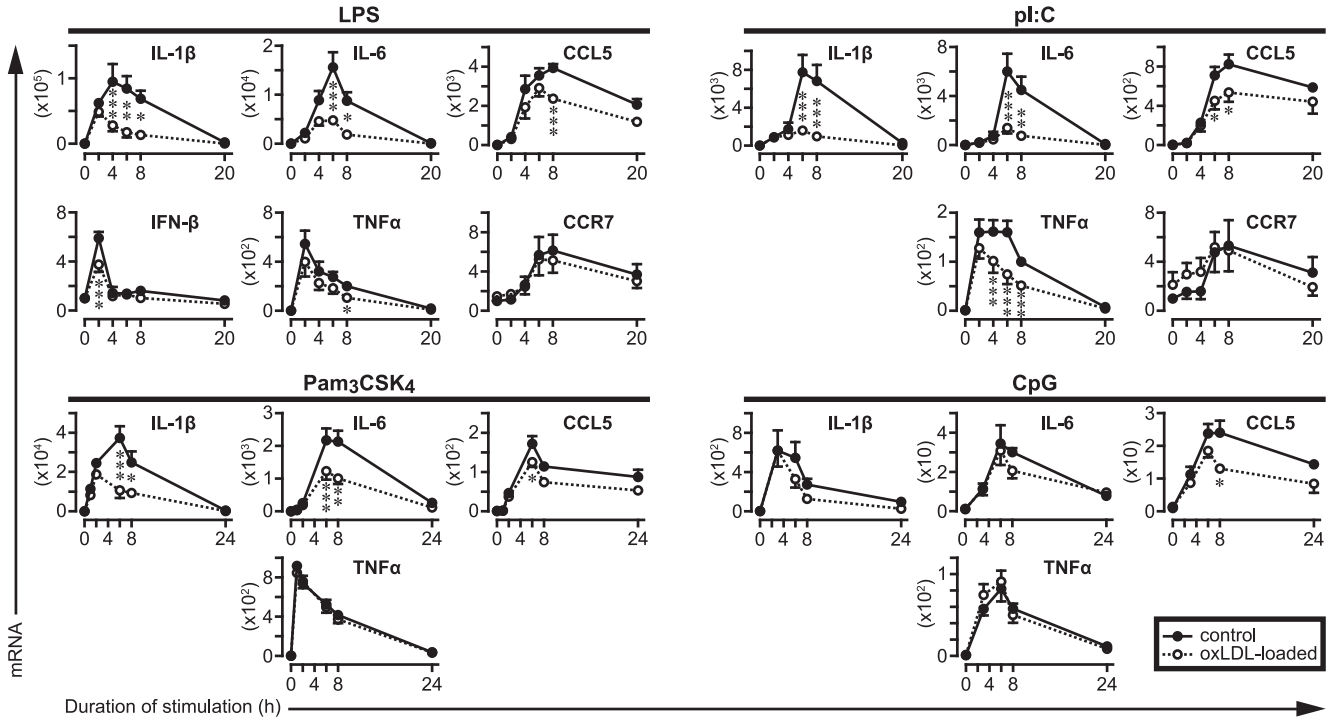

FIGURE 2. oxLDL loading inhibits LPS-, poly(I:C)-, Pam_3CSK_4-, and CpG-induced proinflammatory gene expression. PMϕs were cultured with oxLDL (100 μg/ml, 24 h, ○) or without (control, ●) prior to stimulation with LPS (100 ng/ml, $n = 4$), poly(I:C) (100 μg/ml, $n = 4$), Pam_3CSK_4 (10 ng/ml, $n = 4$), or CpG (300 nM, $n = 3$). mRNA levels (mean ± SEM) were assessed by qPCR and are plotted as fold increase relative to unstimulated control cells (time 0). Significant differences between oxLDL-loaded and corresponding control cells are indicated: $*p < 0.05$, $**p < 0.01$, $***p < 0.001$.

stimulating PMϕs, mRNA levels of most of the proinflammatory genes tested were induced rapidly but to a different extent (Fig. 2). oxLDL loading inhibited LPS-induced IFN-β induction at this early time point, consistent with a previous report (53); however, oxLDL did not have a significant effect on induction of other genes by any of the TLR agonists tested. Induced expression of most proinflammatory genes persisted for at least 8 h. oxLDL loading inhibited expression of IL-1β, IL-6, and CCL5 at 4, 6, and 8 h time points, but it had a modest effect on CpG-induced IL-1β and IL-6. Inhibition of TNF mRNA levels was dependent on the inflammatory stimulus: pronounced in poly(I:C)-treated cells, modest after LPS, and not observed after Pam_3CSK_4 and CpG. LPS- and poly(I:C)-induced CCR7 expression was not affected by oxLDL loading.

We investigated whether oxLDL loading of other myeloid cells inhibits gene expression and found that LPS-induced expression of

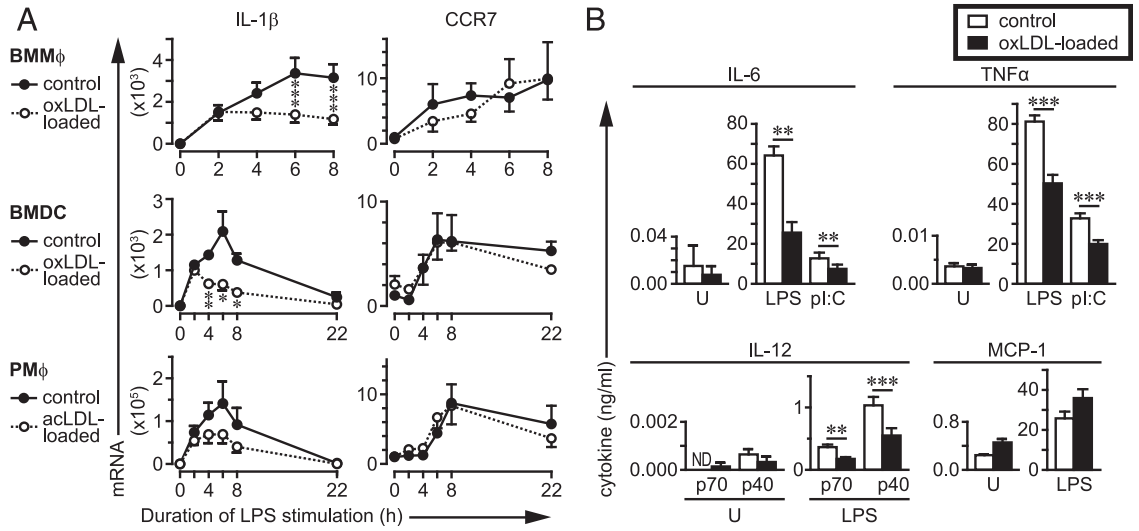

FIGURE 3. (**A**) oxLDL or acLDL loading reduces LPS-induced IL-1β but not CCR7 mRNA levels in different myeloid cells. BMMϕs, BMDCs, or PMϕs were cultured for 24 h without (control), with oxLDL (100 μg/ml), or with acLDL (100 μg/ml) prior to stimulation with LPS. mRNA data are expressed as in Fig. 2 (mean ± SEM; $n = 4$–6 for BMMϕs; $n = 2$ for BMDCs and PMϕs). Significant differences between oxLDL-loaded and corresponding control cells are indicated: $*p < 0.05$, $**p < 0.01$, $***p < 0.001$. (**B**) Loading by oxLDL inhibits LPS- and poly(I:C)-induced cytokine protein production. Control or oxLDL-loaded PMϕs were cultured unstimulated (U) or were stimulated with LPS or poly(I:C). Cytokine levels in culture supernatants harvested at 6 h for MCP-1 ($n = 4$), at 8 h for IL-6 ($n = 6$) and TNF-α ($n = 3$), and at 24 h for IL-12 ($n = 4$) were assessed by ELISA (mean ± SEM; ND, not detected; $**p < 0.01$, $***p < 0.001$).

IL-1β, but not CCR7, mRNA was inhibited at 6–8 h in BMMϕs and BMDCs (Fig. 3A). Similar to oxLDL, acLDL is taken up by scavenger receptors (54). Loading of PMϕs with acLDL appeared to reduce LPS-induced IL-1β, but not CCR7, mRNA levels analogous to oxLDL (Fig. 3A).

oxLDL loading reduces cytokine production

Inhibition of mRNA expression by oxLDL loading was accompanied by reduced secreted levels of LPS- and poly(I:C)-induced IL-6 and TNF-α into the culture media (Fig. 3B). Additionally, the secreted levels of LPS-induced IL-12(p70) and (p40), but not MCP-1, were reduced in PMϕs by oxLDL loading, in line with a reduction in mRNA levels of the IL-12p40 subunit (54,300 ± 6,400 versus 26,800 ± 4,100; $p < 0.01$; $n = 4$), but not MCP-1 (data not shown). Collectively, our data suggest that loading of Mϕs with modified LDL inhibits ongoing TLR-induced mRNA levels and subsequent protein production in a subset of proinflammatory genes, and this may impact the inflammatory response.

oxLDL inhibits the transcription of LPS-induced proinflammatory genes

Steady-state mRNA levels depend on the rate of mRNA transcription and mRNA stability. hnRNA is the precursor of mRNA and has a very short half-life because it is rapidly spliced into mRNA; therefore, hnRNA levels reflect the rate of transcription (55). We investigated whether oxLDL loading influences transcription by measuring hnRNA levels. oxLDL loading reduced hnRNA levels of IL-1β, IL-6, and CCL5 at 4 and 6 h after LPS (Fig. 4).

NF-κB or MAPK signaling remains intact in oxLDL-loaded Mϕs

The inhibition of LPS-induced transcription by oxLDL may result from diminished upstream signaling, and we investigated the canonical NF-κB signaling pathway, which is known to mediate the upregulation of proinflammatory genes in response to LPS. The RAW264.7 murine Mϕ cell line is readily amenable to transfection (27). Upon confirming that loading with oxLDL had an inhibitory effect on LPS-induced gene expression (Supplemental Fig. 1), RAW264.7 cells were transiently transfected with a NF-κB promoter–luciferase reporter construct. This construct is expressed episomally and is not associated with histones or incorporated into chromosomal DNA; therefore, it is not regulated by epigenetics. LPS stimulation dramatically increased NF-κB luciferase activity at 2 h (100-fold), 6 and 8 h (>200-fold), yet comparable increases were observed in oxLDL-loaded cells (Fig. 5A). LPS-induced NF-κB luciferase reporter activity was also comparable in control and oxLDL-loaded BMMϕs (Fig. 5A). Western blotting of key signaling molecules in the NF-κB pathway supported the above data. The kinetics and magnitude of p65/RelA phosphorylation at Ser^{536} (56–58) and IκBα degradation were comparable in control and oxLDL-loaded RAW264.7 cells (Fig. 5B). Similar results were obtained with PMϕs (Supplemental Fig. 2A).

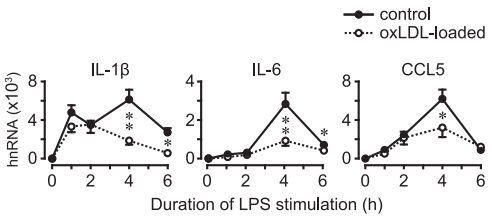

FIGURE 4. oxLDL inhibits LPS-induced transcription. Control or oxLDL-loaded PMϕs were stimulated with LPS as in Fig. 2 and hnRNA levels were determined by qPCR. Data (mean ± SEM; $n = 4$–6) are plotted as fold increase relative to unstimulated control cells (time 0). Significant differences between oxLDL-loaded and corresponding control cells are indicated: *$p < 0.05$, **$p < 0.01$.

LPS also activates three major MAPKs (i.e., ERK, p38, and JNK) that participate in the induction of genes by activation of AP-1 transcription factors (16). Western blotting revealed comparable LPS-induced phosphorylation of ERK, p38, and JNK in control and oxLDL-loaded RAW264.7 cells (Fig. 5C) and PMϕs (Supplemental Fig. 2B). Collectively, our data demonstrated that oxLDL loading does not inhibit TLR4-induced canonical NF-κB and MAPK signaling.

oxLDL loading inhibits LPS-induced binding of p65/RelA subunit of NF-κB to the promoters of IL-6 and CCL5

In addition to signaling, transcription is regulated by epigenetic changes in histones, which organize chromatin and regulate transcription factor accessibility in promoters and enhancers. We employed ChIP assays to determine whether decreased binding of p65 at promoters accounts for reduced TLR4-induced transcription in oxLDL-loaded cells. p65 binding to IL-1β, IL-6, and CCL5 promoters was upregulated 6 h after LPS stimulation (Fig. 6A). In oxLDL-loaded cells, a significant reduction in p65 binding was observed at IL-6 and CCL5 promoters, suggesting that oxLDL loading inhibits LPS-induced epigenetic processes mediating the accessibility of p65 to the promoters of IL-6 and CCL5. The lack of effect of oxLDL on p65 binding to the IL-1β promoter may reflect oxLDL targeting of other transcription factors or other regulatory sequences such as enhancers that bind p65 (59, 60).

HDACs regulate the inhibition of LPS-induced gene expression in oxLDL-loaded RAW264.7 cells

HDACs deacetylate histones and reduce the accessibility of transcription factors to regulatory regions in chromosomal DNA (61). Thus, we investigated whether TSA, a broad-spectrum HDAC inhibitor (61), could modulate the inhibitory effect of oxLDL loading on LPS-induced mRNA expression. We observed that TSA partially rescued the inhibition of LPS-induced IL-1β, IL-6, and CCL5 mRNA in oxLDL-loaded RAW264.7 cells (Fig. 6B).

LXRα/β, PPARγ, and ATF3 are not involved in the regulation of LPS-induced proinflammatory gene expression by oxLDL whereas Nrf2 plays a partial role

We first verified whether LPS-induced IL-1β, IL-6, and CCL5 were affected by LXRα/β deficiency in PMϕs (Supplemental Fig. 3A). The magnitude of proinflammatory gene expression 2 and 6 h after LPS stimulation was mostly comparable in PMϕs isolated from wt and LXRα/β$^{-/-}$ mice; however, a significant reduction between genotypes was observed only for IL-6 at 6 h after LPS. These data suggest that LXR deficiency has a limited effect on LPS-induced gene expression. IL-6 and TNF-α mRNA expression 6 h after LPS was inhibited to the same extent by oxLDL in wt and LXRα/β$^{-/-}$ PMϕs, but a small level of rescue of IL-1β inhibition was seen by LXRα/β deficiency (Fig. 7A). In contrast, LXRα/β deficiency partially reversed the inhibition of LPS-induced expression of all the genes tested by cholesterol-loading of PMϕs at 6 h after LPS (Supplemental Fig. 3B), consistent with a previous report (27). These data suggest that LXRs have differential effects in mediating the inhibition of LPS-induced gene expression in cholesterol-loaded versus oxLDL-loaded cells.

T0070907, a specific antagonist of PPARγ (62), was used to investigate the role of PPARγ in the inhibition of LPS-induced gene expression in oxLDL-loaded cells. T0070907 rescued the

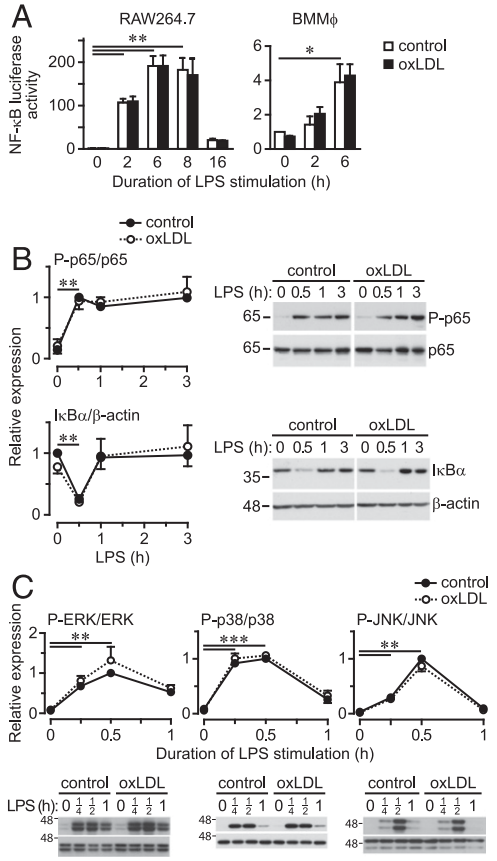

FIGURE 5. oxLDL does not affect LPS-induced NF-κB or MAPK signaling. (**A**) NF-κB reporter activity. RAW264.7 cells or BMMϕs were cotransfected with NF-κB luciferase reporter and the normalizing vectors. Control or oxLDL-loaded cells were stimulated with LPS and luciferase activities were determined. Values represent fold increase relative to unstimulated cells (mean ± SEM; $n = 5$ for RAW264.7; $n = 3$ for BMMϕs; $^{*}p < 0.05$, $^{**}p < 0.01$). (**B**) NF-κB canonical signaling. Control or oxLDL-loaded RAW264.7 cells were stimulated with LPS and whole-cell lysates were analyzed by Western blotting for Ser^{536}p-p65 (P-p65) and IκBα. Representative blots (one of three) are shown. Densitometry data were normalized to total p65 or β-actin levels, respectively. Data are expressed relative to control cells at the 30 min LPS time point for Ser^{536}p-p65, and relative to unstimulated control cells for IκBα (mean ± SEM; $n = 3$; $^{**}p < 0.01$ relative to unstimulated cells). (**C**) MAPK signaling. RAW264.7 cells were treated and analyzed as in (B). Representative blots (one of three) are shown. Densitometry data for p-ERK, p-p38 and p-JNK were normalized to the total corresponding kinase levels. Data are expressed relative to control cells at the 30 min LPS time point (mean ± SEM; $n = 3$; $^{**}p < 0.01$, $^{***}p < 0.001$, relative to unstimulated cells). At each time point, significant differences were not found between control and oxLDL groups when assessing both NF-κB and MAPK signaling.

inhibition of LPS-induced TNF-α expression by rosiglitazone, an agonist of PPARγ (Supplemental Fig. 3C). This inhibitor did not affect the induction of IL-1β, IL-6, and CCL5 genes 6 h after LPS in PMϕs (Supplemental Fig. 3D). Notably, oxLDL-mediated inhibition of LPS-induced expression of these genes was not affected by this antagonist, suggesting that PPARγ is not involved in this process (Fig. 7B).

IL-1β and IL-6 mRNA expression was increased in LPS-treated *Atf3*$^{-/-}$ PMϕs relative to wt (Supplemental Fig. 3E), consistent with the previously recognized role of ATF3 as a negative regulator of TLR4-mediated inflammatory gene expression (41). ATF3 deficiency may enhance oxLDL loading of BMMϕs (39); however, we found that oxLDL loading was lower in *Atf3*$^{-/-}$ PMϕs (Supplemental Fig. 3F). Therefore, we loaded wt PMϕs with 50 μg/ml

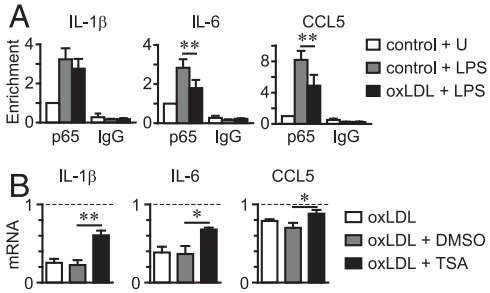

FIGURE 6. (**A**) oxLDL loading reduces the binding of p65/RelA to the promoters of IL-6 and CCL5 in LPS-stimulated RAW264.7 cells. Control and oxLDL-loaded (24 h) RAW cells were left unstimulated (U) or treated with LPS for 6 h. Values derived from ChIP assays represent fold enrichment of p65/RelA on the promoters of genes relative to unstimulated cells (mean ± SEM; $n = 5$; $^{**}p < 0.01$). ChIP assays with nonimmune IgG demonstrate the specificity of the anti-p65 Ab. (**B**) Inhibition of LPS-induced gene expression by oxLDL is partially dependent on HDAC activity. Control and oxLDL-loaded (24 h) RAW264.7 cells were untreated or treated with TSA (50 ng/ml) or DMSO (0.005%, carrier for TSA), and after 15 min stimulated with LPS and cultured for an additional 6 h. The dashed line (assigned a value of 1) represents the LPS-induced expression in control cells (not loaded with oxLDL) for each condition. Normalized mRNA levels in oxLDL-loaded cells were compared (mean ± SEM; $n = 3$; $^{*}p < 0.05$, $^{**}p < 0.01$).

oxLDL to obtain similar loading as in *Atf3*$^{-/-}$ cells with 100 μg/ml oxLDL. IL-1β, IL-6, and CCL5 mRNA expression 6 h after LPS was inhibited by oxLDL loading to the same extent in wt and *Atf3*$^{-/-}$ PMϕs (Fig. 7C), which suggests that ATF3 is not a major player in modulating LPS-induced transcription of proinflammatory genes in oxLDL-loaded cells.

oxLDL loading upregulates antioxidant genes HO-1, SRXN-1, and TXNRD-1 (Fig. 1C), which are targets of NRF2 (48). LPS-induced IL-1β and CCL5 mRNA expression was comparable in wt and *Nrf2*$^{-/-}$ PMϕs, but LPS-induced IL-6 expression was reduced by NRF2 deficiency (Supplemental Fig. 3G). oxLDL loading inhibited LPS-induced IL-6 and CCL5 mRNA expression to a lesser extent in *Nrf2*$^{-/-}$ versus wt PMϕs, and a similar trend was observed for IL-1β (Fig. 7D). These data suggest that NRF2 partially contributes to the inhibition of LPS-induced IL-6, CCL5, and potentially IL-1β expression in oxLDL-loaded cells. To test whether HO-1, an NRF2 target gene, could account for the partial role of NRF2, a specific HO-1 inhibitor, ZnPPIX (63, 64), was added prior to LPS stimulation. ZnPPIX (2 μM) did not influence the extent of LPS-induced IL-1β, IL-6, or CCL5 mRNA levels in oxLDL-loaded PMϕs (data not shown).

Discussion

The relationship between continuous accumulation of foam cells in atherosclerotic plaques and maintenance of chronic inflammation during atherogenesis is not fully understood. In vitro approaches to study the inflammatory status of oxidized lipid-loaded Mϕ yielded controversial results. Whereas some studies have reported minimal or no effects (19, 65), others showed pro- or anti-inflammatory effects of loading with oxLDL (6, 17, 29, 66–72). This may be due to differences in the experimental conditions, including the oxidation levels of LDL particles. In this study, we loaded murine Mϕs with purified oxLDL with a medium level of oxidation. The lipid-loaded Mϕs displayed the characteristic upregulation of CD36 (36) and antioxidant genes (48) (Fig. 1C), as well as the reverse cholesterol-transport genes ABCA1 and ABCG1 (73) (data not shown). We did not observe any proapoptotic effects of oxLDL loading of PMϕs (Fig. 1D). Notably, oxLDL loading was not a proinflammatory

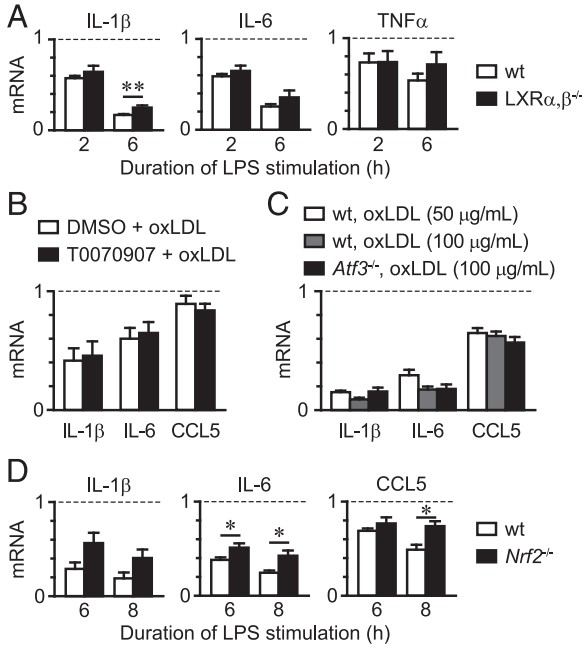

FIGURE 7. Inhibition of LPS-induced gene expression by oxLDL loading is independent of LXR/PPARγ and ATF3, but is partially dependent on NRF2. (**A**) Control and oxLDL-loaded PMϕs from C57BL/6 (wt) and LXRα,β$^{-/-}$ mice were stimulated with LPS. The dashed line (assigned a value of 1) represents mRNA expression in the corresponding control PMϕs (not loaded with oxLDL) for each time point and genotype. Relative mRNA levels in oxLDL-loaded cells are plotted and genotypes were compared (mean ± SEM; n = 4–6 per genotype; $^{**}p < 0.01$). (**B**) PMϕs were treated with T0070907 (10 nM) or DMSO carrier (0.0001%) 1 h prior to 24 h culture without or with oxLDL. Cells were then stimulated with LPS for 6 h. The dashed line represents mRNA expression in PMϕs not loaded with oxLDL [as in (A)] and relative expression in oxLDL-loaded cells is plotted (mean ± SEM; n = 4). Significant differences were not observed between T0070907 and DMSO groups. (**C**) PMϕs from C57BL/6 (wt) and *Atf3*$^{-/-}$ mice were cultured for 24 h without or with oxLDL, prior to stimulation with LPS for 6 h. Data are expressed as in (A) (mean ± SEM; n = 4 per genotype). Significant differences were not observed between wt and *Atf3*$^{-/-}$ groups. (**D**) PMϕs from C57BL/6 (wt) and *Nrf2*$^{-/-}$ mice were cultured for 24 h without or with oxLDL, prior to stimulation with LPS for 6 or 8 h. Data are expressed as in (A) (mean ± SEM; n = 3–5 per genotype). Significant differences were observed between wt and *Nrf2*$^{-/-}$ groups ($^{*}p < 0.05$).

event but rather reduced the inflammatory response when PMϕs were stimulated with LPS, poly(I:C), Pam_3CSK_4, or CpG, ligands for TLR4, TLR3,TLR2/1, or TLR9, respectively (Fig. 2). This effect occurred in a temporal and gene-specific manner. The inhibition of IL-1β, IL-6, and CCL5 mRNA occurred with all agonists and TNF-α mainly with poly(I:C), after the initial induction phase, whereas LPS- or poly(I:C)-induced CCR7 was not inhibited. Thus, our data suggest that rather than affecting early induction, oxLDL loading of Mϕs targets specific TLR-induced mechanisms that are required for the maintenance of induced expression of a subset of proinflammatory genes. The analysis of hnRNA implicated reduced transcription (Fig. 4).

TLR4-mediated induction of gene expression depends on two major signaling cascades that are characterized by the assembly of distinct adaptors, MyD88 and TRAM-TRIF (16). MyD88 initiates signaling proximal to the plasma membrane, whereas TRAM-TRIF signaling emanates from endosomes after TLR4 internalization and has been associated with a later stage of TLR4 signaling (74). TLR3 is localized in endosomes and signals only through TRIF (75). TLR9 localizes in the endoplasmic reticulum and TLR2/1 on the plasma membrane and both receptors signal through MyD88 (26). Thus, it appears that the inhibitory effect by oxLDL does not depend on the TLR-proximal adaptors. Because oxLDL inhibited the expression of a proinflammatory gene subset by all these TLRs, the mechanisms targeted by oxLDL likely involve events that are common to the gene subset and downstream of the TLR-proximal adaptors.

Many proinflammatory genes, including IL-1β, IL-6, and CCL5, contain NF-κB binding sites in their promoters (76–78). We therefore interrogated whether oxLDL loading had any direct effect on intracellular events leading to NF-κB activation by LPS. We found no evidence that the canonical NF-κB signaling pathway was modulated by oxLDL loading of Mϕs. These findings are in agreement with the effects of the oxidized phospholipid oxPAPC on DC activation (28). Although oxLDL reduced TLR4-induced gene expression similarly to cholesterol and desmosterol (27), the mechanisms used by cholesterol loading versus oxLDL loading appear to be different. Unlike cholesterol, oxLDL did not display a dependence on LXRα/β and did not inhibit NF-κB promoter–reporter activity, inferring that oxLDL loading did not inhibit TLR4-induced NF-κB signal transduction, translocation to the nucleus, and binding to multiple NF-κB sites in the episomal promoter–reporter construct. Notably, oxLDL loading reduced LPS-induced binding of the p65/RelA NF-κB subunit to the native promoters of proinflammatory genes, which are integrated into chromosomal DNA. Overall, our data support a role for oxLDL in targeting epigenetic changes that modify chromatin architecture for NF-κB–dependent transcription of IL-6 and CCL5 genes. Two waves of p65 recruitment to promoters were described in LPS-induced RAW264.7 Mϕs (57). Whereas promoters of certain genes, such as IκBα or MIP2, were poised for binding p65 shortly after stimulation, the accessibility of IL-6 and CCL5 promoters was induced relatively later and followed histone H4 acetylation, one of the covalent modifications of chromatin associated with accessibility of transcription factors (57, 79). Our data with the HDAC inhibitor TSA, which was reported to exacerbate atherosclerosis (80), support the possibility that enhanced HDAC activity by oxLDL may reduce the levels of LPS-induced acetylation on histones(s) located at the promoters of IL-6 and CCL5 and thus regulate the accessibility to p65/RelA. Inhibition of the LPS-induced inflammatory response in DCs by oxPAPC was accompanied by reduced phosphorylation of histone H3 (28). The nature of the epigenetic mechanism(s) by which oxLDL loading regulates TLR-induced proinflammatory gene expression will be the subject of future investigations.

Mϕs respond to environmental cues and polarize across a wide spectrum. A proinflammatory M1 phenotype is at one end of this spectrum and an inflammation-resolving and repairing M2 phenotype is at the other end. The Mox phenotype, a response to oxidative stress, is characterized by upregulated expression of antioxidant genes under the regulatory control of NRF2 (48). As expected, we detected significant upregulation of these antioxidant genes by oxLDL, which were further induced by LPS (data not shown). In contrast, the expression of Arg1 and MRC1, markers of the M2 phenotype, were not changed by oxLDL loading (data not shown), suggesting that oxLDL loading leads to the development of Mox but not M2 Mϕ phenotype. Our data support a partial involvement of NRF2 in the regulation of gene expression by oxLDL. Kuhn et al. (81) previously reported a critical role of NRF2 in the regulation of LPS-induced IL-1β and IL-6 expression in oxLDL-loaded Mϕ through HO-1–mediated inhibition of reactive oxygen species production. However, another study did not support such a role for HO-1 (82). Our data using the same inhibitor

of HO-1 as in the above study by Kuhn et al. did not support any role for HO-1 in mediating the inhibitory effects of oxLDL on LPS-induced gene expression. Cross-talk mechanisms between NF-κB and NRF2 pathways have been reported, although they have not been fully elucidated (44, 83–85). Future studies will investigate the potential role of NRF2 in oxLDL-mediated regulation of p65 binding to the promoters of IL-6 and CCL5 in LPS-stimulated cells.

The reduction of the inflammatory response by loading of Mϕs with oxLDL may seem counterintuitive to the existing understanding of atherogenesis. However, the demonstration of time- and gene-dependent effects described in the present study suggests that oxLDL loading may serve as an adaptive mechanism for foam cells to dampen their inflammatory response as part of the maintenance of a chronic atherogenic state in lesions.

Acknowledgments

We thank Dr. Tsonwin Hai (Ohio State University) for providing *Atf3*$^{-/-}$ mice and Dr. Vivek Rao (University Health Network) for providing *Nrf2*$^{-/-}$ mice. We appreciate the assistance of Dr. Nathan Spann (University of California San Diego) with ChIP assays, Dr. Mark Roufaiel and Kaveh Farrokhi with flow cytometry, Haiyan Xiao with mouse husbandry, and Ricky Tsai and Adil Rasheed with husbandry of LXRα/β$^{-/-}$ mice.

Disclosures

The authors have no financial conflicts of interest.

References

1. Libby, P., P. M. Ridker, and A. Maseri. 2002. Inflammation and atherosclerosis. *Circulation* 105: 1135–1143.
2. Steinberg, D. 2009. The LDL modification hypothesis of atherogenesis: an update. *J. Lipid Res.* 50(Suppl.): S376–S381.
3. Bobryshev, Y. V. 2006. Monocyte recruitment and foam cell formation in atherosclerosis. *Micron* 37: 208–222.
4. Paulson, K. E., S. N. Zhu, M. Chen, S. Nurmohamed, J. Jongstra-Bilen, and M. I. Cybulsky. 2010. Resident intimal dendritic cells accumulate lipid and contribute to the initiation of atherosclerosis. *Circ. Res.* 106: 383–390.
5. Zhu, S. N., M. Chen, J. Jongstra-Bilen, and M. I. Cybulsky. 2009. GM-CSF regulates intimal cell proliferation in nascent atherosclerotic lesions. *J. Exp. Med.* 206: 2141–2149.
6. Hjerpe, C., D. Johansson, A. Hermansson, G. K. Hansson, and X. Zhou. 2010. Dendritic cells pulsed with malondialdehyde modified low density lipoprotein aggravate atherosclerosis in Apoe$^{-/-}$ mice. *Atherosclerosis* 209: 436–441.
7. Moore, K. J., and I. Tabas. 2011. Macrophages in the pathogenesis of atherosclerosis. *Cell* 145: 341–355.
8. Gautier, E. L., T. Huby, J. L. Witztum, B. Ouzilleau, E. R. Miller, F. Saint-Charles, P. Aucouturier, M. J. Chapman, and P. Lesnik. 2009. Macrophage apoptosis exerts divergent effects on atherogenesis as a function of lesion stage. *Circulation* 119: 1795–1804.
9. Landsman, L., L. Bar-On, A. Zernecke, K. W. Kim, R. Krauthgamer, E. Shagdarsuren, S. A. Lira, I. L. Weissman, C. Weber, and S. Jung. 2009. CX3CR1 is required for monocyte homeostasis and atherogenesis by promoting cell survival. *Blood* 113: 963–972.
10. Brown, M. S., and J. L. Goldstein. 1979. Receptor-mediated endocytosis: insights from the lipoprotein receptor system. *Proc. Natl. Acad. Sci. USA* 76: 3330–3337.
11. Krieger, M., and J. Herz. 1994. Structures and functions of multiligand lipoprotein receptors: macrophage scavenger receptors and LDL receptor-related protein (LRP). *Annu. Rev. Biochem.* 63: 601–637.
12. Seimon, T., and I. Tabas. 2009. Mechanisms and consequences of macrophage apoptosis in atherosclerosis. *J. Lipid Res.* 50(Suppl.): S382–S387.
13. Caligiuri, G., J. Khallou-Laschet, M. Vandaele, A. T. Gaston, S. Delignat, C. Mandet, H. V. Kohler, S. V. Kaveri, and A. Nicoletti. 2007. Phosphorylcholine-targeting immunization reduces atherosclerosis. *J. Am. Coll. Cardiol.* 50: 540–546.
14. Tsimikas, S., A. Miyanohara, K. Hartvigsen, E. Merki, P. X. Shaw, M. Y. Chou, J. Pattison, M. Torzewski, J. Sollors, T. Friedmann, et al. 2011. Human oxidation-specific antibodies reduce foam cell formation and atherosclerosis progression. *J. Am. Coll. Cardiol.* 58: 1715–1727.
15. Lu, Y. C., W. C. Yeh, and P. S. Ohashi. 2008. LPS/TLR4 signal transduction pathway. *Cytokine* 42: 145–151.
16. Ostuni, R., I. Zanoni, and F. Granucci. 2010. Deciphering the complexity of Toll-like receptor signaling. *Cell. Mol. Life Sci.* 67: 4109–4134.
17. Stewart, C. R., L. M. Stuart, K. Wilkinson, J. M. van Gils, J. Deng, A. Halle, K. J. Rayner, L. Boyer, R. Zhong, W. A. Frazier, et al. 2010. CD36 ligands promote sterile inflammation through assembly of a Toll-like receptor 4 and 6 heterodimer. *Nat. Immunol.* 11: 155–161.
18. Wiesner, P., S. H. Choi, F. Almazan, C. Benner, W. Huang, C. J. Diehl, A. Gonen, S. Butler, J. L. Witztum, C. K. Glass, and Y. I. Miller. 2010. Low doses of lipopolysaccharide and minimally oxidized low-density lipoprotein cooperatively activate macrophages via nuclear factor κB and activator protein-1: possible mechanism for acceleration of atherosclerosis by subclinical endotoxemia. *Circ. Res.* 107: 56–65.
19. Ohlsson, B. G., M. C. Englund, A. L. Karlsson, E. Knutsen, C. Erixon, H. Skribeck, Y. Liu, G. Bondjers, and O. Wiklund. 1996. Oxidized low density lipoprotein inhibits lipopolysaccharide-induced binding of nuclear factor-kappaB to DNA and the subsequent expression of tumor necrosis factor-alpha and interleukin-1beta in macrophages. *J. Clin. Invest.* 98: 78–89.
20. Michelsen, K. S., M. H. Wong, P. K. Shah, W. Zhang, J. Yano, T. M. Doherty, S. Akira, T. B. Rajavashisth, and M. Arditi. 2004. Lack of Toll-like receptor 4 or myeloid differentiation factor 88 reduces atherosclerosis and alters plaque phenotype in mice deficient in apolipoprotein E. *Proc. Natl. Acad. Sci. USA* 101: 10679–10684.
21. Coenen, K. R., M. L. Gruen, R. S. Lee-Young, M. J. Puglisi, D. H. Wasserman, and A. H. Hasty. 2009. Impact of macrophage Toll-like receptor 4 deficiency on macrophage infiltration into adipose tissue and the artery wall in mice. *Diabetologia* 52: 318–328.
22. Lundberg, A. M., D. F. Ketelhuth, M. E. Johansson, N. Gerdes, S. Liu, M. Yamamoto, S. Akira, and G. K. Hansson. 2013. Toll-like receptor 3 and 4 signalling through the TRIF and TRAM adaptors in haematopoietic cells promotes atherosclerosis. *Cardiovasc. Res.* 99: 364–373.
23. Boekholdt, S. M., W. R. Agema, R. J. Peters, A. H. Zwinderman, E. E. van der Wall, P. H. Reitsma, J. J. Kastelein, and J. W. Jukema, Regression Growth Evaluation Statin Study Group. 2003. Variants of Toll-like receptor 4 modify the efficacy of statin therapy and the risk of cardiovascular events. *Circulation* 107: 2416–2421.
24. Kiechl, S., E. Lorenz, M. Reindl, C. J. Wiedermann, F. Oberhollenzer, E. Bonora, J. Willeit, and D. A. Schwartz. 2002. Toll-like receptor 4 polymorphisms and atherogenesis. *N. Engl. J. Med.* 347: 185–192.
25. Hodgkinson, C. P., and S. Ye. 2011. Toll-like receptors, their ligands, and atherosclerosis. *Sci. World J.* 11: 437–453.
26. Roshan, M. H., A. Tambo, and N. P. Pace. 2016. The Role of TLR2, TLR4, and TLR9 in the pathogenesis of atherosclerosis. *Int. J. Inflamm.* 2016: 1532832.
27. Spann, N. J., L. X. Garmire, J. G. McDonald, D. S. Myers, S. B. Milne, N. Shibata, D. Reichart, J. N. Fox, I. Shaked, D. Heudobler, et al. 2012. Regulated accumulation of desmosterol integrates macrophage lipid metabolism and inflammatory responses. *Cell* 151: 138–152.
28. Blüml, S., G. Zupkovitz, S. Kirchberger, M. Seyerl, V. N. Bochkov, K. Stuhlmeier, O. Majdic, G. J. Zlabinger, C. Seiser, and J. Stöckl. 2009. Epigenetic regulation of dendritic cell differentiation and function by oxidized phospholipids. *Blood* 114: 5481–5489.
29. Habets, K. L., G. H. van Puijvelde, L. M. van Duivenvoorde, E. J. van Wanrooij, P. de Vos, J. W. Tervaert, T. J. van Berkel, R. E. Toes, and J. Kuiper. 2010. Vaccination using oxidized low-density lipoprotein-pulsed dendritic cells reduces atherosclerosis in LDL receptor-deficient mice. *Cardiovasc. Res.* 85: 622–630.
30. Shamshiev, A. T., F. Ampenberger, B. Ernst, L. Rohrer, B. J. Marsland, and M. Kopf. 2007. Dyslipidemia inhibits Toll-like receptor-induced activation of CD8α-negative dendritic cells and protective Th1 type immunity. *J. Exp. Med.* 204: 441–452.
31. Bensinger, S. J., and P. Tontonoz. 2008. Integration of metabolism and inflammation by lipid-activated nuclear receptors. *Nature* 454: 470–477.
32. Lehmann, J. M., S. A. Kliewer, L. B. Moore, T. A. Smith-Oliver, B. B. Oliver, J. L. Su, S. S. Sundseth, D. A. Winegar, D. E. Blanchard, T. A. Spencer, and T. M. Willson. 1997. Activation of the nuclear receptor LXR by oxysterols defines a new hormone response pathway. *J. Biol. Chem.* 272: 3137–3140.
33. Janowski, B. A., P. J. Willy, T. R. Devi, J. R. Falck, and D. J. Mangelsdorf. 1996. An oxysterol signalling pathway mediated by the nuclear receptor LXRα. *Nature* 383: 728–731.
34. Chawla, A., W. A. Boisvert, C. H. Lee, B. A. Laffitte, Y. Barak, S. B. Joseph, D. Liao, L. Nagy, P. A. Edwards, L. K. Curtiss, et al. 2001. A PPARγ-LXR-ABCA1 pathway in macrophages is involved in cholesterol efflux and atherogenesis. *Mol. Cell* 7: 161–171.
35. Ghisletti, S., W. Huang, S. Ogawa, G. Pascual, M. E. Lin, T. M. Willson, M. G. Rosenfeld, and C. K. Glass. 2007. Parallel SUMOylation-dependent pathways mediate gene- and signal-specific transrepression by LXRs and PPARγ. *Mol. Cell* 25: 57–70.
36. Nagy, L., P. Tontonoz, J. G. Alvarez, H. Chen, and R. M. Evans. 1998. Oxidized LDL regulates macrophage gene expression through ligand activation of PPARγ. *Cell* 93: 229–240.
37. Welch, J. S., M. Ricote, T. E. Akiyama, F. J. Gonzalez, and C. K. Glass. 2003. PPARγ and PPARδ negatively regulate specific subsets of lipopolysaccharide and IFN-γ target genes in macrophages. *Proc. Natl. Acad. Sci. USA* 100: 6712–6717.
38. Zhao, W., L. Wang, M. Zhang, P. Wang, L. Zhang, C. Yuan, J. Qi, Y. Qiao, P. C. Kuo, and C. Gao. 2011. Peroxisome proliferator-activated receptor γ negatively regulates IFN-β production in Toll-like receptor (TLR) 3- and TLR4-stimulated macrophages by preventing interferon regulatory factor 3 binding to the IFN-β promoter. *J. Biol. Chem.* 286: 5519–5528.
39. Gold, E. S., S. A. Ramsey, M. J. Sartain, J. Selinummi, I. Podolsky, D. J. Rodriguez, R. L. Moritz, and A. Aderem. 2012. ATF3 protects against atherosclerosis by suppressing 25-hydroxycholesterol-induced lipid body formation. *J. Exp. Med.* 209: 807–817.

40. Hai, T., C. C. Wolford, and Y. S. Chang. 2010. ATF3, a hub of the cellular adaptive-response network, in the pathogenesis of diseases: is modulation of inflammation a unifying component? *Gene Expr.* 15: 1–11.
41. Gilchrist, M., V. Thorsson, B. Li, A. G. Rust, M. Korb, J. C. Roach, K. Kennedy, T. Hai, H. Bolouri, and A. Aderem. 2006. Systems biology approaches identify ATF3 as a negative regulator of Toll-like receptor 4. [Published erratum appears in 2008 *Nature* 451: 1022.] *Nature* 441: 173–178.
42. Reboldi, A., E. V. Dang, J. G. McDonald, G. Liang, D. W. Russell, and J. G. Cyster. 2014. Inflammation. 25-Hydroxycholesterol suppresses interleukin-1–driven inflammation downstream of type I interferon. *Science* 345: 679–684.
43. Barajas, B., N. Che, F. Yin, A. Rowshanrad, L. D. Orozco, K. W. Gong, X. Wang, L. W. Castellani, K. Reue, A. J. Lusis, and J. A. Araujo. 2011. NF-E2–related factor 2 promotes atherosclerosis by effects on plasma lipoproteins and cholesterol transport that overshadow antioxidant protection. *Arterioscler. Thromb. Vasc. Biol.* 31: 58–66.
44. Buelna-Chontal, M., and C. Zazueta. 2013. Redox activation of Nrf2 & NF-κB: a double end sword? *Cell. Signal.* 25: 2548–2557.
45. Collins, A. R., A. A. Gupte, R. Ji, M. R. Ramirez, L. J. Minze, J. Z. Liu, M. Arredondo, Y. Ren, T. Deng, J. Wang, et al. 2012. Myeloid deletion of nuclear factor erythroid 2–related factor 2 increases atherosclerosis and liver injury. *Arterioscler. Thromb. Vasc. Biol.* 32: 2839–2846.
46. Kiefer, F., J. Brumell, N. Al-Alawi, S. Latour, A. Cheng, A. Veillette, S. Grinstein, and T. Pawson. 1998. The Syk protein tyrosine kinase is essential for Fcγ receptor signaling in macrophages and neutrophils. *Mol. Cell. Biol.* 18: 4209–4220.
47. Xu, Y., Y. Zhan, A. M. Lew, S. H. Naik, and M. H. Kershaw. 2007. Differential development of murine dendritic cells by GM-CSF versus Flt3 ligand has implications for inflammation and trafficking. *J. Immunol.* 179: 7577–7584.
48. Kadl, A., A. K. Meher, P. R. Sharma, M. Y. Lee, A. C. Doran, S. R. Johnstone, M. R. Elliott, F. Gruber, J. Han, W. Chen, et al. 2010. Identification of a novel macrophage phenotype that develops in response to atherogenic phospholipids via Nrf2. *Circ. Res.* 107: 737–746.
49. Boullier, A., Y. Li, O. Quehenberger, W. Palinski, I. Tabas, J. L. Witztum, and Y. I. Miller. 2006. Minimally oxidized LDL offsets the apoptotic effects of extensively oxidized LDL and free cholesterol in macrophages. *Arterioscler. Thromb. Vasc. Biol.* 26: 1169–1176.
50. Wintergerst, E. S., J. Jelk, C. Rahner, and R. Asmis. 2000. Apoptosis induced by oxidized low density lipoprotein in human monocyte-derived macrophages involves CD36 and activation of caspase-3. *Eur. J. Biochem.* 267: 6050–6059.
51. Yan, H., S. Wang, Z. Li, Z. Sun, J. Zan, W. Zhao, Y. Pan, Z. Wang, M. Wu, and J. Zhu. 2016. Rspo2 suppresses CD36-mediated apoptosis in oxidized low density lipoprotein-induced macrophages. *Mol. Med. Rep.* 14: 2945–2952.
52. Tsutsumi, S., T. Gotoh, W. Tomisato, S. Mima, T. Hoshino, H. J. Hwang, H. Takenaka, T. Tsuchiya, M. Mori, and T. Mizushima. 2004. Endoplasmic reticulum stress response is involved in nonsteroidal anti-inflammatory drug-induced apoptosis. *Cell Death Differ.* 11: 1009–1016.
53. Marson, A., R. M. Lawn, and T. Mikita. 2004. Oxidized low density lipoprotein blocks lipopolysaccharide-induced interferon beta synthesis in human macrophages by interfering with IRF3 activation. *J. Biol. Chem.* 279: 28781–28788.
54. Kunjathoor, V. V., M. Febbraio, E. A. Podrez, K. J. Moore, L. Andersson, S. Koehn, J. S. Rhee, R. Silverstein, H. F. Hoff, and M. W. Freeman. 2002. Scavenger receptors class A-I/II and CD36 are the principal receptors responsible for the uptake of modified low density lipoprotein leading to lipid loading in macrophages. *J. Biol. Chem.* 277: 49982–49988.
55. Elferink, C. J., and J. J. Reiners, Jr. 1996. Quantitative RT-PCR on CYP1A1 heterogeneous nuclear RNA: a surrogate for the in vitro transcription run-on assay. *Biotechniques* 20: 470–477.
56. Mathes, E., E. L. O'Dea, A. Hoffmann, and G. Ghosh. 2008. NF-κB dictates the degradation pathway of IκBα. *EMBO J.* 27: 1357–1367.
57. Saccani, S., S. Pantano, and G. Natoli. 2001. Two waves of nuclear factor κB recruitment to target promoters. *J. Exp. Med.* 193: 1351–1359.
58. Schmitz, M. L., S. Bacher, and M. Kracht. 2001. IκB-independent control of NF-κB activity by modulatory phosphorylations. *Trends Biochem. Sci.* 26: 186–190.
59. Brown, J. D., C. Y. Lin, Q. Duan, G. Griffin, A. J. Federation, R. M. Paranal, S. Bair, G. Newton, A. H. Lichtman, A. L. Kung, et al. 2014. NF-κB directs dynamic super enhancer formation in inflammation and atherogenesis. *Mol. Cell* 56: 219–231.
60. Zhang, Y., S. Saccani, H. Shin, and B. S. Nikolajczyk. 2008. Dynamic protein associations define two phases of IL-1β transcriptional activation. *J. Immunol.* 181: 503–512.
61. de Ruijter, A. J., A. H. van Gennip, H. N. Caron, S. Kemp, and A. B. van Kuilenburg. 2003. Histone deacetylases (HDACs): characterization of the classical HDAC family. *Biochem. J.* 370: 737–749.
62. Yano, M., T. Matsumura, T. Senokuchi, N. Ishii, Y. Murata, K. Taketa, H. Motoshima, T. Taguchi, K. Sonoda, D. Kukidome, et al. 2007. Statins activate peroxisome proliferator-activated receptor γ through extracellular signal-regulated kinase 1/2 and p38 mitogen-activated protein kinase-dependent cyclooxygenase-2 expression in macrophages. *Circ. Res.* 100: 1442–1451.
63. Józkowicz, A., and J. Dulak. 2003. Effects of protoporphyrins on production of nitric oxide and expression of vascular endothelial growth factor in vascular smooth muscle cells and macrophages. *Acta Biochim. Pol.* 50: 69–79.
64. Hirai, K., T. Sasahira, H. Ohmori, K. Fujii, and H. Kuniyasu. 2007. Inhibition of heme oxygenase-1 by zinc protoporphyrin IX reduces tumor growth of LL/2 lung cancer in C57BL mice. *Int. J. Cancer* 120: 500–505.
65. Walton, K. A., A. L. Cole, M. Yeh, G. Subbanagounder, S. R. Krutzik, R. L. Modlin, R. M. Lucas, J. Nakai, E. J. Smart, D. K. Vora, and J. A. Berliner. 2003. Specific phospholipid oxidation products inhibit ligand activation of Toll-like receptors 4 and 2. *Arterioscler. Thromb. Vasc. Biol.* 23: 1197–1203.
66. Sheedy, F. J., A. Grebe, K. J. Rayner, P. Kalantari, B. Ramkhelawon, S. B. Carpenter, C. E. Becker, H. N. Ediriweera, A. E. Mullick, D. T. Golenbock, et al. 2013. CD36 coordinates NLRP3 inflammasome activation by facilitating intracellular nucleation of soluble ligands into particulate ligands in sterile inflammation. *Nat. Immunol.* 14: 812–820.
67. Fong, L. G., T. A. Fong, and A. D. Cooper. 1991. Inhibition of lipopolysaccharide-induced interleukin-1β mRNA expression in mouse macrophages by oxidized low density lipoprotein. *J. Lipid Res.* 32: 1899–1910.
68. Hamilton, J. A., D. Myers, W. Jessup, F. Cochrane, R. Byrne, G. Whitty, and S. Moss. 1999. Oxidized LDL can induce macrophage survival, DNA synthesis, and enhanced proliferative response to CSF-1 and GM-CSF. *Arterioscler. Thromb. Vasc. Biol.* 19: 98–105.
69. Perrin-Cocon, L., F. Coutant, S. Agaugué, S. Deforges, P. André, and V. Lotteau. 2001. Oxidized low-density lipoprotein promotes mature dendritic cell transition from differentiating monocyte. *J. Immunol.* 167: 3785–3791.
70. Chung, S. W., B. Y. Kang, S. H. Kim, Y. K. Pak, D. Cho, G. Trinchieri, and T. S. Kim. 2000. Oxidized low density lipoprotein inhibits interleukin-12 production in lipopolysaccharide-activated mouse macrophages via direct interactions between peroxisome proliferator-activated receptor-γ and nuclear factor-κB. *J. Biol. Chem.* 275: 32681–32687.
71. Jiang, Y., M. Wang, K. Huang, Z. Zhang, N. Shao, Y. Zhang, W. Wang, and S. Wang. 2012. Oxidized low-density lipoprotein induces secretion of interleukin-1β by macrophages via reactive oxygen species-dependent NLRP3 inflammasome activation. *Biochem. Biophys. Res. Commun.* 425: 121–126.
72. Liu, W., Y. Yin, Z. Zhou, M. He, and Y. Dai. 2014. OxLDL-induced IL-1β secretion promoting foam cells formation was mainly via CD36 mediated ROS production leading to NLRP3 inflammasome activation. *Inflamm. Res.* 63: 33–43.
73. Li, A. C., C. J. Binder, A. Gutierrez, K. K. Brown, C. R. Plotkin, J. W. Pattison, A. F. Valledor, R. A. Davis, T. M. Willson, J. L. Witztum, et al. 2004. Differential inhibition of macrophage foam-cell formation and atherosclerosis in mice by PPARα, β/δ, and γ. *J. Clin. Invest.* 114: 1564–1576.
74. Kagan, J. C., T. Su, T. Horng, A. Chow, S. Akira, and R. Medzhitov. 2008. TRAM couples endocytosis of Toll-like receptor 4 to the induction of interferon-β. *Nat. Immunol.* 9: 361–368.
75. Meylan, E., K. Burns, K. Hofmann, V. Blancheteau, F. Martinon, M. Kelliher, and J. Tschopp. 2004. RIP1 is an essential mediator of Toll-like receptor 3-induced NF-κB activation. *Nat. Immunol.* 5: 503–507.
76. Anrather, J., G. Racchumi, and C. Iadecola. 2005. *cis*-Acting, element-specific transcriptional activity of differentially phosphorylated nuclear factor-κB. *J. Biol. Chem.* 280: 244–252.
77. Génin, P., M. Algarté, P. Roof, R. Lin, and J. Hiscott. 2000. Regulation of RANTES chemokine gene expression requires cooperativity between NF-κB and IFN-regulatory factor transcription factors. *J. Immunol.* 164: 5352–5361.
78. Liang, M. D., Y. Zhang, D. McDevit, S. Marecki, and B. S. Nikolajczyk. 2006. The interleukin-1β gene is transcribed from a poised promoter architecture in monocytes. *J. Biol. Chem.* 281: 9227–9237.
79. Pons, D., F. R. de Vries, P. J. van den Elsen, B. T. Heijmans, P. H. Quax, and J. W. Jukema. 2009. Epigenetic histone acetylation modifiers in vascular remodelling: new targets for therapy in cardiovascular disease. *Eur. Heart J.* 30: 266–277.
80. Choi, J. H., K. H. Nam, J. Kim, M. W. Baek, J. E. Park, H. Y. Park, H. J. Kwon, O. S. Kwon, D. Y. Kim, and G. T. Oh. 2005. Trichostatin A exacerbates atherosclerosis in low density lipoprotein receptor-deficient mice. *Arterioscler. Thromb. Vasc. Biol.* 25: 2404–2409.
81. Kuhn, A. M., N. Tzieply, M. V. Schmidt, A. von Knethen, D. Namgaladze, M. Yamamoto, and B. Brüne. 2011. Antioxidant signaling via Nrf2 counteracts lipopolysaccharide-mediated inflammatory responses in foam cell macrophages. *Free Radic. Biol. Med.* 50: 1382–1391.
82. Min, K. J., K. H. Cho, and T. K. Kwon. 2012. The effect of oxidized low density lipoprotein (oxLDL)-induced heme oxygenase-1 on LPS-induced inflammation in RAW 264.7 macrophage cells. *Cell. Signal.* 24: 1215–1221.
83. Cuadrado, A., Z. Martín-Moldes, J. Ye, and I. Lastres-Becker. 2014. Transcription factors NRF2 and NF-κB are coordinated effectors of the Rho family, GTP-binding protein RAC1 during inflammation. *J. Biol. Chem.* 289: 15244–15258.
84. Liu, G. H., J. Qu, and X. Shen. 2008. NF-κB/p65 antagonizes Nrf2-ARE pathway by depriving CBP from Nrf2 and facilitating recruitment of HDAC3 to MafK. *Biochim. Biophys. Acta* 1783: 713–727.
85. Lv, P., P. Xue, J. Dong, H. Peng, R. Clewell, A. Wang, Y. Wang, S. Peng, W. Qu, Q. Zhang, et al. 2013. Keap1 silencing boosts lipopolysaccharide-induced transcription of interleukin 6 via activation of nuclear factor κB in macrophages. *Toxicol. Appl. Pharmacol.* 272: 697–702.